Robotica (2008) volume 26, pp. 93–98. © 2007 Cambridge University Press
doi:10.1017/S0263574707003621 Printed in the United Kingdom

Dynamic dexterity of a planar 2-DOF parallel manipulator in a hybrid machine tool

Jun Wu*, Jinsong Wang, Tiemin Li, Liping Wang and Liwen Guan

Institute of Manufacturing Engineering, Department of Precision Instruments and Mechanology, Tsinghua University, Beijing 100084, P. R. China.

(Received in Final Form: May 24, 2007. First published online: July 12, 2007)

SUMMARY

This paper addresses the dynamic dexterity of a planar 2-degree of freedom (DOF) parallel manipulator with virtual constraint. Without simplification, the dynamic formulation is derived by using the virtual work principle. The condition number of the inertia matrix of the dynamic equation is presented as a criterion to evaluate the dynamic dexterity of a manipulator. In order to obtain the best isotropic configuration of the dynamic dexterity in the whole workspace, two global performance indices, which consider the mean value and standard deviation of the condition number of the inertia matrix, respectively, are proposed as the objective function. For a given set of geometrical and inertial parameters, the dynamic dexterity of the parallel manipulator is more isotropic in the center than at the boundaries of the workspace.

KEYWORDS: Dynamic dexterity; Parallel manipulator; Dynamic formulation; Condition number.

1. Introduction

The development of dynamic models for parallel manipulators is important in several different ways. First, a dynamic model can be used for computer simulation of a robotic system. Second, it can be used for the development of suitable control strategies. Third, the dynamic analysis reveals all the joint reaction forces and moments necessary for sizing the links, bearings, and actuators. Several approaches have been proposed for dynamic modeling.[1–3] For the planar 2-degree of freedom (DOF) parallel manipulator studied in this paper, there are a few manipulators with identical structure.[4–6] Due to the virtual constraint architecture, in previous work, the two links of one kinematic chain was simplified as one link in dynamic modeling. Then, the Newton–Euler approach was used to derive the dynamic equation. This method cannot lead to a compact form of the dynamic equation, which is necessary for investigating the dynamic dexterity.

It is important to consider the dynamic dexterity for problems of manipulator design [7]. The dynamic dexterity is an evaluation of the efficiency and easiness for performing the required manipulator tasks. Some measures for evaluating dynamic dexterity have been proposed. Dynamic manipulability[8–11] can deal with weights of directions using maximum required accelerations. However, there are some disadvantages. For example, the directions are limited to those coordinate axes in which the acceleration is not required such that there is no direction, and the evaluation standard value cannot be maintained at an invariable value when the weights change according to the progress of a task. In [12,13], it has been demonstrated that a new definition of the force manipulability ellipsoid is necessary for redundant manipulators. Asada[14,15] has presented the manipulator dynamics in the task space by constructing a generalized inertia ellipsoid (GIE) at each point of the workspace. The change in shape and orientation of the GIE from point-to-point in the workspace was related to the nonlinear forces and coupling in the manipulator dynamics.

The harmonic mean of the square singular values of the inertia matrix can evaluate the dynamic dexterity.[7] When it becomes difficult to accelerate the end-effector in a direction, a singular value approaches zero. Then, the measure always has a small value, since the term of the smallest singular value becomes dominant. However, when there is a direction in which the end-effector can be hardly accelerated, it does not always have bad value if it can be easily accelerated in other directions. The smallest singular value of inertia matrix of a manipulator can be used for the evaluation when the dexterity in the hardest direction is considered.[16] However, the dynamic dexterity is not considered in all directions.

In this paper, utilizing the virtual work principle, the dynamic model of a planar 2-DOF parallel manipulator with virtual constraint is derived. Based on the relationship between the actuated joint forces and the acceleration of the moving platform, the condition number of inertia matrix of dynamic equation is proposed for evaluating the dynamic dexterity of a manipulator. Furthermore, two global conditioning indices are developed. As a result, the dynamic dexterity of the planar parallel manipulator is more isotropic in the center than at the boundaries of the workspace.

2. Structure Description and Kinematic Analysis

2.1. Structure description of the hybrid machine tool

The hybrid machine tool with five DOFs is designed to machine huge blades and guide vanes of hydraulic turbine generator sets. Since the machine tool is very large, the stiffness will be low if the conventional serial structure is employed. Thus, a parallel manipulator is adopted. By

* Corresponding author. E-mail: wu-j03@mails.tsinghua.edu.cn.

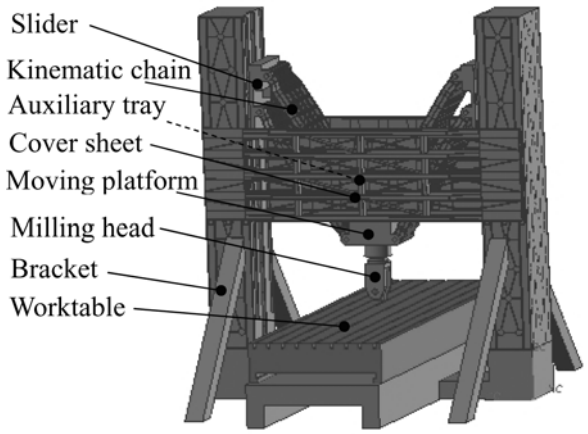

Fig. 1. Prototype of the hybrid machine tool.

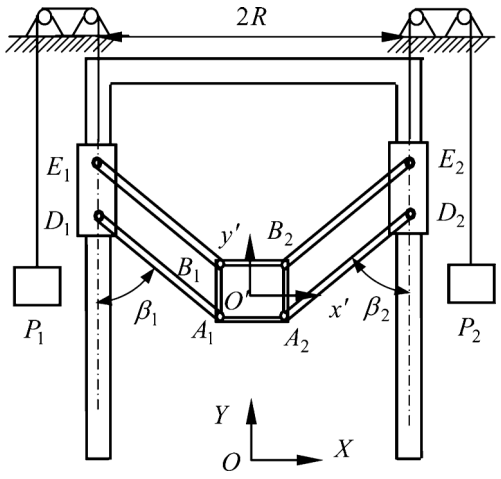

Fig. 2. The kinematic model.

combining the parallel manipulator with a feed worktable and a 2-DOF rotating head, the machine tool is created, as shown in Fig. 1. In this paper, we mainly study the dynamic dexterity of the parallel manipulator.

2.2. *Structure description of the parallel manipulator*

As shown in Fig. 2, the parallel manipulator is composed of a gantry frame, a moving platform, two active sliders, and two kinematic chains. Each chain consists of a parallelogram. The parallel manipulator is virtually constraint, since one of the four links can be removed without affecting the kinematics of the manipulator. In order to improve the loading and accelerating capability of servomotors, counterweights P_1 and P_2 (see Fig. 2) are connected to sliders E_1D_1 and E_2D_2, respectively. Sliders E_1D_1 and E_2D_2 drive the two kinematic chains when they slide along the vertical guide ways; and the sliders are driven by the servomotors via leads screw. Thus, the moving platform possesses a 2-DOF translational moving capability in a plane.

2.3. *Inverse kinematics*

In the practical application, the planar parallel manipulator is a subpart of a hybrid machine tool. Thus, the base coordinate system O–XY shown in Fig. 2 is identical with the real machine coordinate system of the hybrid machine tool such that the kinematic model can be applied directly into the control system. A moving coordinate system O'–$x'y'$, which is parallel to O–XY is fixed at the center of the moving platform. Let the position vector of the origin O' be $\boldsymbol{r}_{O'} = [x\ y]^{\mathrm{T}}$ in the base coordinate system; and the position vectors of point A_i and B_i $(i = 1, 2)$ can be expressed as

$$\boldsymbol{r}_{Ai} = [x_{Ai} \quad y_{Ai}]^{\mathrm{T}} = \boldsymbol{r}'_O + \boldsymbol{r}'_{Ai}, \qquad i = 1, 2 \tag{1}$$

$$\boldsymbol{r}_{Bi} = [x_{Bi} \quad y_{Bi}]^{\mathrm{T}} = \boldsymbol{r}'_O + \boldsymbol{r}'_{Bi}, \qquad i = 1, 2 \tag{2}$$

where $\boldsymbol{r}'_{Ai}$ and $\boldsymbol{r}'_{Bi}$ are the position vectors of points A_i and B_i in the coordinate system O'–$x'y'$, and $\boldsymbol{r}'_{\mathrm{A1}} = [-r\ -h]^{\mathrm{T}}$, $\boldsymbol{r}'_{\mathrm{A2}} = [r\ -h]^{\mathrm{T}}$, $\boldsymbol{r}'_{\mathrm{B1}} = [-r\ h]^{\mathrm{T}}$, $\boldsymbol{r}'_{\mathrm{B2}} = [r\ h]^{\mathrm{T}}$ and h and r are the half of the height and width of the moving platform, respectively.

According to Fig. 2, the following equations can be obtained.

$$\sin\beta_i = \frac{x_{\mathrm{A}i} - x_{\mathrm{D}i}}{l}, \quad \cos\beta_i = \frac{y_{\mathrm{D}i} - y_{\mathrm{A}i}}{l}, \qquad i = 1, 2 \tag{3}$$

where l is the length of the link, β_i is the angle between link A_iD_i and the vertical axis parallel to the Y-axis, $0 \le \beta_1 \le \pi$ and $-\pi \le \beta_2 \le 0$.

From Eq. (3), the inverse kinematic solutions of the manipulator can be written as

$$q_1 = y_{\mathrm{D1}} = y - h \pm \sqrt{l^2 - (x - r + R)^2} \tag{4a}$$

$$q_2 = y_{\mathrm{D2}} = y - h \pm \sqrt{l^2 - (x + r - R)^2}. \tag{4b}$$

It can be concluded that the singularity occurs when one of the four links is in a horizontal position and/or one link of the kinematic chain is parallel to one link of the other chain. In the practical application, the singularity should be avoided. To avoid the singularity, it is obvious that $0 < |\beta_i| < \frac{\pi}{2}$. Thus, for the configuration shown in Fig. 2, the "±" of Eq. (4) should be '+'.

2.4. *Jacobian matrix*

Taking the time derivative of Eq. (3) leads to

$$\dot{\beta}_i = \dot{x}/(l\cos\beta_i) \tag{5}$$

$$\dot{q}_i = \dot{y} - \tan\beta_i \cdot \dot{x} = \boldsymbol{J}_i[\dot{x}\ \ \dot{y}]^{\mathrm{T}} \tag{6}$$

where $\boldsymbol{J}_i = [-\tan\beta_i \ \ 1]$.

Equation (6) can be rewritten as

$$\dot{\boldsymbol{q}} = \boldsymbol{J}\,\dot{\boldsymbol{p}} \tag{7}$$

where $\dot{\boldsymbol{q}} = [\dot{q}_1\ \dot{q}_2]^T$, $\dot{\boldsymbol{p}} = [\dot{x}\ \dot{y}]^T$ is the velocity of the moving platform, $\boldsymbol{J}$ is the Jacobian matrix, and $\boldsymbol{J} = [\boldsymbol{J}_1^T\ \boldsymbol{J}_2^T]^T$.

2.5. *Partial velocity matrix and partial angular velocity matrix*

In order to obtain a more compact form of the dynamic model, the virtual work principle is employed to derive the dynamic model. Thus, the partial velocity and partial angular velocity matrices, which are used in dynamic modeling, should be determined first. To find the partial velocity matrix,

https://doi.org/10.1017/S0263574707003621 Published online by Cambridge University Press

a pivotal point should be selected to have the simplest form of velocity such that the determination of partial velocity matrix can be most efficient. For example, the point D_i is selected as the pivotal point of slider E_iD_i and link A_iD_i, and E_i is the pivotal point of link B_iE_i. The mass centers of the counterweight and the moving platform are regarded as their pivotal points. Then, the partial velocity matrix of each pivotal point and partial angular velocity matrix of each moving part can be computed, respectively.

Since the slider has only the translational capability, the partial angular velocity matrix can be expressed as

$$\boldsymbol{G}_{i1} = 0. \tag{8}$$

According to Eq. (6), the partial velocity matrix of point D_i is given by

$$\boldsymbol{H}_{i1} = [0 \;\; 1]^T \boldsymbol{J}_i. \tag{9}$$

Based on Eq. (5), the partial angular velocity matrix of link A_iD_i and partial velocity matrix of point D_i can be written as

$$\boldsymbol{G}_{i2} = \begin{bmatrix} \dfrac{1}{\cos\beta_i \cdot l} & 0 \end{bmatrix} \tag{10}$$

$$\boldsymbol{H}_{i2} = \boldsymbol{H}_{i1}. \tag{11}$$

Due to the parallelogram of each kinematic chain, the motion of link B_iE_i is the same as that of link A_iD_i. Thus, the partial velocity matrix of point E_i and the partial angular velocity matrix of link B_iE_i are the same as those of point D_i and link A_iD_i. So that

$$\boldsymbol{G}_{i3} = \boldsymbol{G}_{i2}, \quad \boldsymbol{H}_{i3} = \boldsymbol{H}_{i2}. \tag{12}$$

Since the counterweight is connected to the slider, the velocity of the counterweight is negative of that of the slider. Then, based on Eq. (6), the partial angular velocity matrix and partial velocity matrix of the mass center of the counterweight can be expressed, respectively, as

$$\boldsymbol{G}_{i4} = 0, \quad \boldsymbol{H}_{i4} = [\,0 \quad -1\,]^{\mathrm{T}} \boldsymbol{J}_i. \tag{13}$$

Considering that the moving platform cannot rotate, the partial angular velocity matrix of the moving platform and partial velocity matrix of point O' are given by

$$\boldsymbol{G}_N = 0 \tag{14}$$

$$\boldsymbol{H}_N = \begin{bmatrix} 1 & 0 \\ 0 & 1 \end{bmatrix}. \tag{15}$$

3. Dynamic Modeling Based on Virtual Work Principle

3.1. Acceleration analysis

Taking the time derivative of Eqs. (5) and (6) leads to

$$\ddot{\beta}_i = \frac{\ddot{x}}{l\cos\beta_i} + \frac{\dot{x}^2 \sin\beta_i}{l^2\cos^3\beta_i} \tag{16}$$

$$\ddot{q}_i = \ddot{y} - \frac{\sin\beta_i}{\cos\beta_i}\ddot{x} - \frac{\dot{x}^2\sin^2\beta_i}{l\cos^3\beta_i} - \dot{\beta}_i^2 l\cos\beta_i. \tag{17}$$

Thus, the accelerations of point E_i and D_i are determined by

$$\boldsymbol{a}_{Ei} = \boldsymbol{a}_{Di} = [0 \;\; 1]^{\mathrm{T}}\ddot{q}_i. \tag{18}$$

3.2. Inertial forces and moments of moving parts

Utilizing the Newton–Euler formulation, the inertial force and moment of each moving part about its pivotal point can be determined. Here, we denote that m_{i1}, m_{i2}, m_{i3}, m_{i4} and m_N are the masses of the slider, links A_iD_i and B_iE_i, the counterweight and the moving platform, respectively, $\boldsymbol{g}$ is the gravitational acceleration vector and $\boldsymbol{g} = [0 \quad -9.8]^{\mathrm{T}}$.

The inertial force and moment of the slider about point E_i can be expressed as

$$\boldsymbol{F}_{i1} = -m_{i1}(\boldsymbol{a}_{Ei} - \boldsymbol{g}) = -m_{i1}\begin{bmatrix} 0 \\ \ddot{y} - \tan\beta_i\ddot{x} \end{bmatrix} + \tilde{\boldsymbol{F}}_{i1} \tag{19}$$

$$M_{i1} = 0. \tag{20}$$

where

$$\tilde{\boldsymbol{F}}_{i1} = m_{i1}\begin{bmatrix} 0 \\ \dfrac{\dot{x}^2\sin^2\beta_i}{l\cos^3\beta_i} + \dot{\beta}_i^2 l\cos\beta_i \end{bmatrix} + m_{i1}\boldsymbol{g}.$$

The inertial force and moment of link A_iD_i about point D_i can be expressed as

$$\begin{aligned} \boldsymbol{F}_{i2} =& \\ & -m_{i2}\left(\boldsymbol{a}_{Di} + s_{i2}\ddot{\beta}_i\boldsymbol{E}\begin{bmatrix}\sin\beta_i \\ -\cos\beta_i\end{bmatrix} - s_{i2}\dot{\beta}_i^2\begin{bmatrix}\sin\beta_i \\ -\cos\beta_i\end{bmatrix} - \boldsymbol{g}\right) \\ & = -m_{i2}\begin{bmatrix} s_{i2}\ddot{x}/l \\ \ddot{y} - \tan\beta_i\ddot{x} + s_{i2}/l\cdot\tan\beta_i\ddot{x}\end{bmatrix} + \tilde{\boldsymbol{F}}_{i2} \end{aligned} \tag{21}$$

$$\begin{aligned} M_{i2} &= -\ddot{\beta}_i I_{i2} + m_{i2}s_{i2}[\sin\beta_i - \cos\beta_i]\boldsymbol{E}(\boldsymbol{a}_{Di} - \boldsymbol{g}) \\ &= \frac{m_{i2}s_{i2}\sin^2\beta_i - I_{i2}}{l\cos\beta_i}\ddot{x} - m_{i2}s_{i2}\sin\beta_i\ddot{y} + \tilde{M}_{i2} \end{aligned} \tag{22}$$

where

$$\boldsymbol{E} = \begin{bmatrix} 0 & -1 \\ 1 & 0 \end{bmatrix},$$

$$\begin{aligned} \tilde{\boldsymbol{F}}_{i2} = & \; m_{i2}\begin{bmatrix} 0 \\ \dot{x}^2\sin^2\beta_i/(l\cos^3\beta_i) + \dot{\beta}_i^2 l\cos\beta_i \end{bmatrix} + m_{i2}\boldsymbol{g} \\ & + m_{i2}s_{i2}\dot{\beta}_i^2\begin{bmatrix}\sin\beta_i \\ -\cos\beta_i\end{bmatrix} - m_{i2}s_{i2}\frac{\dot{x}^2\sin\beta_i}{l^2\cos^3\beta_i}\begin{bmatrix}\sin\beta_i \\ -\cos\beta_i\end{bmatrix} \end{aligned}$$

$$\begin{aligned} \tilde{M}_{i2} = & \frac{m_{i2}s_{i2}l\sin^2\beta_i - I_{i2}\sin^2\beta_i}{l^2\cos^3\beta_i}\dot{x}^2 \\ & + m_{i2}s_{i2}\beta_i^2 l\cos\beta_i - 9.8\cdot m_{i2}s_{i2}, \end{aligned}$$

$\boldsymbol{a}_{Di}$ is the acceleration of point D_i, s_{i2} is the distance between the mass center of link A_iD_i and point D_i, and I_{i2} is the moment of inertia of link A_iD_i about point D_i.

Since the motion of link B_iE_i is the same as that of link A_iD_i, the inertial force and moment of link B_iE_i are the

https://doi.org/10.1017/S0263574707003621 Published online by Cambridge University Press

same as those of link A_iD_i. Thus, we have

$$\boldsymbol{F}_{i3} = \boldsymbol{F}_{i2} \tag{23}$$

$$M_{i3} = M_{i2} \tag{24}$$

The inertial force and moment of the counterweight about its mass center can be written as

$$\boldsymbol{F}_{i4} = -m_{i4}\,(\boldsymbol{a}_{Pi} - \boldsymbol{g}) = m_{i4}\begin{bmatrix} 0 \\ \ddot{y} - \tan\boldsymbol{\beta}_i\ddot{x} \end{bmatrix} + \tilde{\boldsymbol{F}}_{i4} \tag{25}$$

$$M_{i4} = 0 \tag{26}$$

where

$$\tilde{\boldsymbol{F}}_{i4} = m_{i4}\begin{bmatrix} 0 \\ -\dot{\beta}_i^2 l\cos\beta_i - \dfrac{\dot{x}^2\sin^2\beta_i}{(l\cos^3\beta_i)\tan\ddot{x}} \end{bmatrix} + m_{i4}g,$$

$\boldsymbol{a}_{Pi}$ is the acceleration of the counterweight, and it is the negative of $\boldsymbol{a}_{Ei}$.

The inertial force and moment of the moving platform about point O' can be expressed as

$$\boldsymbol{F}_N = -m_N(\boldsymbol{a} - \boldsymbol{g}) \tag{27}$$

$$M_N = 0 \tag{28}$$

where $\boldsymbol{a}$ is the acceleration of origin O' and $\boldsymbol{a} = [\ddot{x}\ \ \ddot{y}]^{\mathrm{T}}$.

3.3. Dynamic model

Based on the virtual work principle, the dynamic formulation of the parallel manipulator can be expressed as

$$\boldsymbol{J}^{\mathrm{T}}\boldsymbol{\tau} + \sum_{i=1}^{2}\sum_{j=1}^{4}\begin{bmatrix}\boldsymbol{H}_{ij}^{\mathrm{T}} & \mathbf{G}_{ij}^{\mathrm{T}}\end{bmatrix}\begin{bmatrix}\boldsymbol{F}_{ij} \\ M_{ij}\end{bmatrix} + \begin{bmatrix}\boldsymbol{H}_N^{\mathrm{T}} & \boldsymbol{G}_N^{\mathrm{T}}\end{bmatrix}\begin{bmatrix}\boldsymbol{F}_N \\ M_N\end{bmatrix} = 0 \tag{29}$$

where $\boldsymbol{\tau} = [F_1\ \ F_2]^{\mathrm{T}}$, and F_1, F_2 are the driving forces that act on sliders E_1D_1 and E_2D_2, respectively. Equation (29) can be rewritten as

$$\boldsymbol{\tau} = \boldsymbol{J}^{-\mathrm{T}}\boldsymbol{M}\,(\boldsymbol{a})\,\boldsymbol{a} + \boldsymbol{N} \tag{30}$$

where

$$\boldsymbol{M}\,(\boldsymbol{a}) = -\sum_{i=1}^{2}\left(\begin{array}{l} -m_{i1}\begin{bmatrix}\tan^2\beta_i & -\tan\beta_i \\ -\tan\beta_i & 1\end{bmatrix} \\ -2m_{i2}\begin{bmatrix}\tan^2\beta_i\,(1 - s_{i2}/l) & -\tan\beta_i \\ \tan\beta_i s_{i2}/l - \tan\beta_i & 1\end{bmatrix} \\ +2\begin{bmatrix}0 & 0 \\ \dfrac{m_{i2}s_{i2}l\sin\beta_i - I_{i2}}{l\cos^2\beta_i} & \dfrac{-m_{i2}s_{i2}}{\cos\beta_i}\end{bmatrix} \\ +m_{i4}\begin{bmatrix}-\tan^2\beta_i & \tan\beta_i \\ \tan\beta_i & -1\end{bmatrix} \end{array}\right)$$

$$+ m_N\begin{bmatrix}1 & 0 \\ 0 & 1\end{bmatrix}$$

$$N = -\sum_{i=1}^{2}\left(\begin{array}{l}\begin{bmatrix}0 & -\tan\beta_i \\ 0 & 1\end{bmatrix}\tilde{\boldsymbol{F}}_{i1} + 2\begin{bmatrix}0 & -\tan\beta_i \\ 0 & 1\end{bmatrix}\tilde{\boldsymbol{F}}_{i2} \\ +2\begin{bmatrix}1/(l\cos\beta_i) \\ 0\end{bmatrix}\tilde{M}_{i2} + \begin{bmatrix}0 & \tan\beta_i \\ 0 & -1\end{bmatrix}\tilde{\boldsymbol{F}}_{i4}\end{array}\right), \quad - m_N\boldsymbol{g}$$

and $\boldsymbol{N}$ consists of the centrifugal, coriolis, and gravitational forces.

4. Dynamic Dexterity Evaluation

Conventionally, the generalized inertia ellipsoid has been proposed for evaluating the dynamic performance of a manipulator. As addressed in [8], the dynamic performance of a high-speed manipulator can be represented by the degree of arbitrariness of changing the acceleration on the actuated joint force. Thus, rewriting Eq. (30) in a unified form by neglecting $\boldsymbol{N}$, leads to

$$\boldsymbol{\tau} \approx \boldsymbol{J}^{-\mathrm{T}}\boldsymbol{M}(\boldsymbol{a})\boldsymbol{a} \tag{31}$$

where $\boldsymbol{J}^{-\mathrm{T}}\boldsymbol{M}(\boldsymbol{a})$ is the inertia matrix.

Based on the generalized inertia ellipsoid, it can be concluded that the moving platform can be easily accelerated in the direction of major axis of this ellipsoid. In the direction of minor axis, it can be hardly accelerated. If the lengths of the principal axes are the same, the accelerating performance is isotropic. Namely, the dynamic dexterity is best. The difference between the lengths of major and minor axes stands for the anisotropy of the accelerating performance.

In the dynamic optimum design, if the issue that the accelerating/decelerating capabilities along all directions should be more isotropic is considered, the condition number of the inertia matrix of the dynamic equation, i.e., κ_D, is proposed to quantify the dynamic dexterity of manipulators. κ_D is defined as

$$1 \le \kappa_D = \frac{\sigma_2}{\sigma_1} \le \infty \tag{32}$$

where σ_1 and σ_2 are the minimum and maximum singular values of the inertia matrix with a given posture.

The dynamic condition number κ_D can evaluate the dynamic dexterity when the difference between the easiest direction and the hardest direction is the main issue. Furthermore, considering that κ_D varies in different configurations of the manipulator, one of the two global indices, similar to that introduced in,[17,18] is proposed as

$$\bar{\eta}_D = \frac{\int_{W_t}\kappa_D dW_t}{\int_{W_t} dW_t} \tag{33}$$

where W_t is the task workspace of a manipulator in which the dynamic dexterity is evaluated. The geometrical meaning of $\bar{\eta}_D$ can be interpreted as the mean value of κ_D in W_t. Due to its incapability of reflecting the fluctuation of κ_D, another

https://doi.org/10.1017/S0263574707003621 Published online by Cambridge University Press

conditioning index is introduced

$$\tilde{\eta}_D = \frac{\sqrt{\int_{W_t} (\kappa_D - \bar{\eta}_D)^2 \, dW_t}}{\int_{W_t} dW_t} \tag{34}$$

where $\tilde{\eta}_D$ is the standard deviation of κ_D with respect to its mean value $\bar{\eta}_D$ in W_t. It is certain that $\tilde{\eta}_D$ should be minimized for achieving a better dynamic dexterity.

In dynamic design, the design parameters (kinematic parameters, mass distribution, etc.) are optimized by minimizing the objective function $\bar{\eta}_D$ or $\tilde{\eta}_D$ such that the dynamic dexterity is more isotropic.

5. Numerical Simulation

As an example to investigate the dynamic dexterity, the geometrical and inertial parameters of the parallel manipulator are given in Table I.

The task workspace of the manipulator is a rectangle with width 3 m and height 1.8 m. The distance between the lower boundary of the task workspace and the Y-axis is 1 m. Let the moving platform move from the point with the coordinate (−1.5 m, 2 m) to another point with the coordinate (1.5 m, 2 m). The driving forces are shown in Fig. 3. It can be seen that driving forces F_1 and F_2 acting on sliders E_1D_1 and E_2D_2 are symmetrical with the Y-axis when the moving platform moves along a symmetrical trajectory about the Y-axis.

Figure 4 shows the generalized inertia ellipsoid. The moving platform can possess a maximum (minimum) acceleration in the direction of the major (minor) axis of the ellipsoid. The larger is the area of ellipsoid, the larger is the output acceleration. From Fig. 4, it can be seen that the distribution of the generalized inertia ellipsoid are symmetrical with respect to the Y-axis. This means that the accelerating capability is symmetrical about the Y-axis. Moreover, the accelerating capability of the point in the Y-axis is maximum along the Y-axis direction and minimum along the X-axis direction.

Table I. The geometrical and inertial parameters.

Parameter	Value	Parameter	Value
m_{11}	2836 kg	m_{24}	9672 kg
m_{21}	2836 kg	m_N	5000 kg
m_{12}	2168 kg	r	0.55 m
m_{22}	2168 kg	R	2.342 m
m_{13}	2168 kg	l	3.55 m
m_{23}	2168 kg	I_{12}	9107.4 kg · m^2
m_{14}	9672 kg	I_{22}	9107.4 kg · m^2

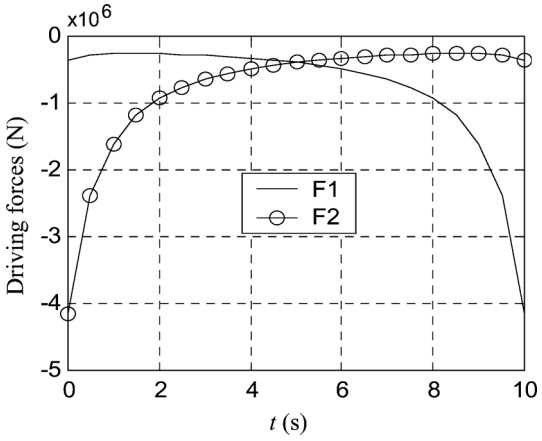

Fig. 3. The driving forces.

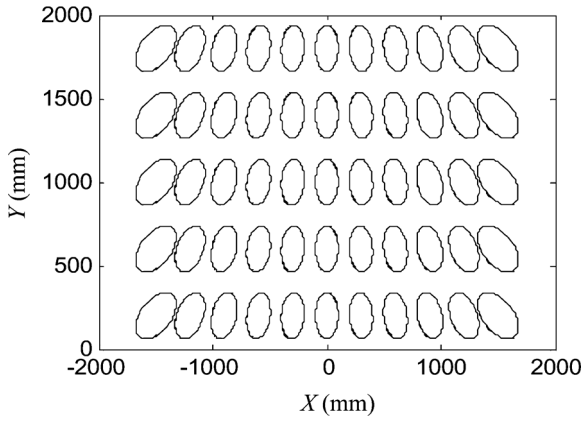

Fig. 4. Disrtibution of generalized inertia ellipsoid.

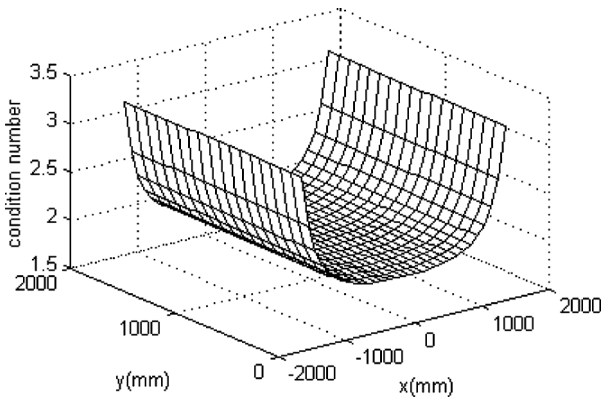

Fig. 5. Condition number of the inertia matrix.

Figure 5 is the condition number of the inertia matrix in the dynamic equation of the 2-DOF parallel manipulator in the workspace. It can be seen that the condition number of the inertia matrix is also symmetrical about the Y-axis; and the dynamic dexterity is more isotropic in the center than at the boundaries of the workspace. In the Y-axis, κ_D is smallest and the dynamic dexterity is most isotropic.

Furthermore, in order to investigate the validity of the proposed performance indices κ_D and $\bar{\eta}_D$ for evaluating the dynamic dexterity, the virtual constrained link E_1B_1 is disassembled. The dynamic dexterity of the manipulator without link E_1B_1 is shown in Fig. 6. It can be seen that the condition number of the inertia matrix of the manipulator without link E_1B_1 is not symmetrical about the Y-axis any more. The isotropy of dynamic dexterity of the manipulator without link E_1B_1 is worse than that of the manipulator discussed in this paper.

https://doi.org/10.1017/S0263574707003621 Published online by Cambridge University Press

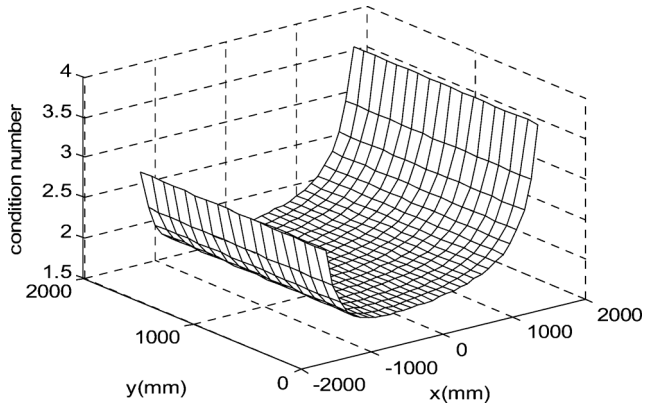

Fig. 6. Condition number of the inertia matrix with link E_1B_1 omitted.

6. Conclusions

This paper derives the dynamic formulation of a planar 2-DOF parallel manipulator and investigates the dynamic dexterity. The conclusions are drawn as follows:

(i) Without simplification, the dynamic equation of the parallel manipulator with virtual constraint is obtained by using the virtual work principle.

(ii) The condition number of the inertia matrix of dynamic equation is presented as a criterion to evaluate the dynamic dexterity of a manipulator. In order to obtain the maximum isotropy of dynamic dexterity in the workspace, $\bar{\eta}_D$ and $\tilde{\eta}_D$ are proposed in terms of the mean value and standard deviation of κ_D.

(iii) The accelerating capability of the parallel manipulator is symmetrical with respect to the Y-axis, and the accelerating capability of the point in the Y-axis is maximum along the Y-axis direction and minimum along the X-axis direction. The dynamic condition number of the inertia matrix is also symmetrical about the Y-axis; and the dynamic dexterity is more isotropic in the center than at the boundaries of the workspace.

Acknowledgments

This work was supported by the 863 High-Tech Scheme (Grant No. 2004AA424120 and 2005AA424223), the "973" key fundamental programs of China (Grant No. 2004CB318007 and 2006CB705400), and the National Nature Science Foundation of China (Grant No. 50605041). The authors would like to thank Professor Xin-Jun Liu for the discussion on the paper.

References

1. B. Dasgupta, T. S. Mruthyunjaya, "A Newton–Euler formulation for the inverse dynamics of the stewart platform manipulator," *Mech. Mach. Theory* **33**(8), 1135–1152 (1998).
2. C. D. Zhang, S. M. Song, "An efficient method for inverse dynamics of manipulators based on the virtual work principle," *J. Robot. Syst.* **10**(5), 605–627 (1993).
3. Y. Li, Q. Xu, "Kinematics and inverse dynamics analysis for a general 3-PRS spatial parallel mechanism," *Robotica* **23**(2), 219–229 (2005).
4. L.-P. Wang, J.-S. Wang and J. Chen, "The dynamic analysis of a 2-PRR planar parallel mechanism," *Proc. Inst. Mech. Engrs. C: J. Mech. Eng. Sci.* **219**(9), 901–909 (2005).
5. L. P. Wang, J. S. Wang, Y. W. Li and Y. Lu, "Kinematic and dynamic equations of a planar parallel manipulator," *Proc. Inst. Mech. Engrs. C: J. Mech. Eng. Sci.* **217**(5), 525–531 (2003).
6. J. Wu, J. Wang, T. Li and L. Wang, "Analysis and application of a 2-DOF planar parallel mechanism," *ASME J. Mech. Design* **129**(4), 434–437 (2007).
7. S. Tadokoro, I. Kimura and T. Takamori, "A measure for evaluation of dynamic dexterity based on a stochastic interpretation of manipulator motion," *Proceedings of the Fifth International Conference on Advanced Robotics* (1991) pp. 509–514.
8. T. Yoshikawa, "Dynamic manipulability of robot manipulators," *J. Robot. Syst.* **2**(1), 113–124 (1985).
9. T. Yoshikawa, "Manipulability of robotic mechanisms," *Int. J. Robot. Res.* **4**(2), 3–9 (1985).
10. F. C. Park and J. W. Kim, "Manipulability of closed kinematic chains," *ASME J. Mech. Design* **120**(4), 542–548 (1998).
11. X.-J. Liu, Q.-M. Wang and J. Wang "Kinematics, dynamics and dimensional synthesis of a novel 2-DoF translational manipulator," *J. Intell. Robot. Syst.* **41**(4), 205–224 (2005).
12. P. Chiacchio, Y. Bouffard-Vercelli and F. Pierrot, "Force polytope and force ellipsoid for redundant manipulators," *J. Robot. Syst.* **14**(8), 613–620 (1997).
13. P. Chiacchio, "New dynamic manipulability ellipsoid for redundant manipulators," *Robotica* **18**(4), 381–387 (2000).
14. H. Asada, "A geometrical representation of manipulator dynamics and its application to arm design," *J. Dynam. Syst. Meas. Control* **105**(3), 131–135 (1983).
15. H. Asada and K. Youcef-Toumi, "Analysis and design of a direct-drive arm with a five-bar-link parallel drive mechanism," *ASME J. Dynam. Syst. Meas. Control* **106**(3), 225–230 (1984).
16. M. Li, T. Huang, J. Mei *et al.*, "Dynamic formulation and performance comparison of the 3-DOF modules of two reconfigurable PKM-the Tricept and the TriVariant," *ASME J. Mech. Design* **127**(6), 1129–1136 (2005).
17. C. M. Gosselin and J. Angeles, "A global performance index for the kinematic optimization of robotic manipulators," *ASME J. Mech. Design* **113**(3), 220–226 (1991).
18. X.-J. Liu, Z.-L. Jin and F. Gao, "Optimum design of 3-DOF spherical parallel manipulators with respect to the conditioning and stiffness indices," *Mech. Mach. Theory* **35**(9), 1257–1267 (2000).

https://doi.org/10.1017/S0263574707003621 Published online by Cambridge University Press